Mode Switching Smooth Control of Transient Process of Grid-Connected 400 Hz Solid-State Power Supply System

Jun-Jie Zhu[*], Zi-Ling Nie[†], Yin-Feng Zhang[*], and Yi Han[*]

[*],[†]National Key Laboratory for Vessel Integrated Power System Technology,
Naval University of Engineering, Wuhan, China

Abstract

The mode-switching control of transient process is important to grid-connected 400 Hz solid-state power supply systems. Therefore, this paper analyzes the principle of on-grid and islanding operation of the system with or without local loads in the grid-connected process and provides a theoretical study of the effect of different switching sequences on the mode-switching transient process. The conclusion is that the mode switch (MS) must be turned on before the solid-state switch (STS) in the on-grid process and that STS must be turned off before the MS in the off-grid process. A strategy of mode-switching smooth control for transient process of the system is proposed, including its concrete steps. The strategy utilizes the average distribution of peak currents and the smooth adjustment of peak currents and phases to achieve a no-shock grid connection. The simulation and experimental results show that the theoretical analysis is correct and that the method is effective.

Key words: Grid-connected, MS, Smooth control, STS, Transient process, 400 Hz solid-static power supply

I. INTRODUCTION

In recent years, the demand for a 400 Hz power capacity for large ships has been increasing, as a 400-Hz power supply is an essential component of key equipment such as carrier-based aircrafts, missile systems, radars, and sonars. A 400-Hz solid-state power supply of high-level integration can flexibly expand the capacity and increase the reliability of operations [1]-[4].

However, the appropriateness of the mode-switching control of transient process for the grid-connected 400 Hz solid-state power supply system, strongly influences system stability, impulse current, and the service life of itsunits. The seamless switching between the grid units and the power grid ensures power supply continuity of the important loads within the units [5], which plays an important role in the safe and stable operation of the power grid. Meanwhile, mode-switching

control as an important technology of the grid-connected system has received widespread attention [6]-[8].

Much of the research in mode-switching control focuses on power frequency systems, which mainly refers to the switching process between a single inverter or microgrid with the local load and a large power grid [9]-[12]. In [13], a micogrid-connected/islanding seamless switching technique based on energy storage is presented. Using energy storage, the technique could control the seamless transition of the microgrid from an islanding operation mode to a grid-connected operation mode. However, this method could not be directly used for the 400-Hz solid-state power supply system due to the severely weak damping and the added energy storage unit. In [14], a circuit switching method based on UTC4053 was proposed to control the islanding or grid-connected operation modes. This method uses grid-connected and independent operation controls as two input channels. The microcontroller unit (MCU) sends a mode selection signal through UTC4053 to fulfill the selection of either channel. The method is relatively effective for low-power and simple inverters but not for a large-capacity grid-connected 400-Hz solid-state power supply system, as the time delay caused by switching between the channels greatly affects phase synchronization control and

lowers its reliability. Literature [15] investigated the islanding/grid-connected control involved in the single inverter operating with local loads. They offered the mode-switching algorithm based on the self-control method of the inverter. For lack of detailed analysis of the mode-switching transient process, the above papers are all based on power frequency systems. However, research in medium frequency systems involves a greater amount of difficulty in current sharing and phase synchronization controls. For example, the output voltage frequency is eight times that of power frequency. When sampling frequency is 10 kHz, the signal must be sampled 200 times for the power frequency system but only 25 times for the medium frequency system. The active and reactive power values calculated according to the voltage and current data obtained from sampling are less accurate than those of the frequency inverter [16]–[17]. For the power frequency system, the phase difference between the two movements of the switching device is 1.8°, as compared with that of the medium frequency system, which is 14.4°. Consequently, the mode-switching control of transient process becomes more difficult.

This research conducted a theoretical study on the effect of different switching sequences on the mode switching transient process of the grid-connected 400-Hz solid-state power supply system according to the principle of islanding and grid-connected operations with or without local loads in the process of grid integration. The conclusion is that the mode switch (MS) must be turned on before the solid-state switch (STS) in the on-grid process, and STS must be turned off before MS in the off-grid process. Moreover, a novel strategy of mode-switching smooth control is proposed, including its concrete steps. The strategy is used to achieve average distribution of peak currents and smooth adjustment of peak currents and phases to ensure a no-shock grid connection. Simulations and experiments show that the theoretical analysis is correct and that the strategy is effective.

II. OPERATION MODE OF THE GRID-CONNECTED SYSTEM

To analyze the principle of operation mode of the grid-connected system, the topology of the 400-Hz solid-state power supply is shown in Fig. 1. The three-phase four-wire inverter topology of double cascade-connected H-bridges is adopted for the system, with each phase independently controlled. Taking phase A as an example, two H-bridge outputs are connected in a series by the same transformers.

The adoption of the staggered control technique, called carrier phase shift control, between the two H-bridge inverters each taking the mode of frequency-doubling PWM control could make the control system achieve an effect four times that of the switching frequency. Meanwhile, the output
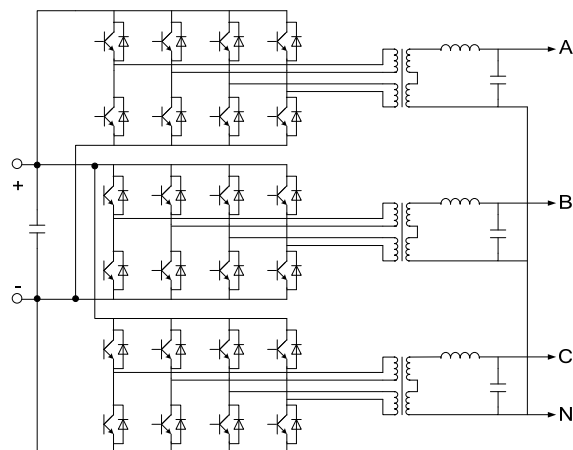

Fig. 1. Topology of three-phase four-wire 400-Hz solid-state power supply.
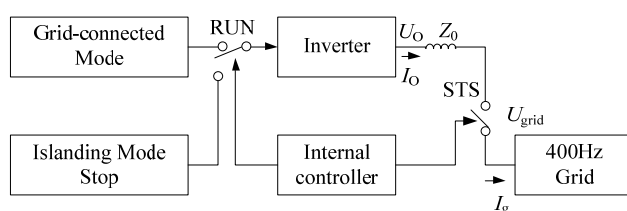

Fig. 2. Principle of the on/off-grid process of the 400-Hz solid-state power supply without local loads.

voltage of the left is generated to increase the degree of freedom of the control. The right bridge leg can be acquired by the carrier pulse width modulation (PWM), which is a five-level converter.

Multilevel carrier phase shifting is used to compare four triangular carrier waves staggering at 90 degrees, with the modulation wave generating four groups of independent PWM modulation signals, which can drive eight power units. As each H-bridge unit regresses to the two-level PWM control, the total output voltage of the two H-bridges generates a five-level equivalent PWM waveform. Thus, the control bandwidth of the system can be improved, which consequently guarantees the quality of the output voltage.

The mode conversion transient process of the grid-connected 400 Hz solid-state power supply system is closely related to its working mode. Dealing with different modes of system operation is necessary to analyze and control the transient process more effectively.

A. On/Off-Grid Process without Local Loads

Figure 2 shows the operating principle of the on/off-grid process of the 400-Hz solid-state power supply without local loads. In this case, the grid-connected system only requires the power supply to work in the grid-connected mode. Thus, control is relatively simple. RUN in the figure is the instruction of the output PWM pulse. In the on-grid process, STS is turned on by an internal controller of the grid unit (the power supply), and the power supply is connected to the grid
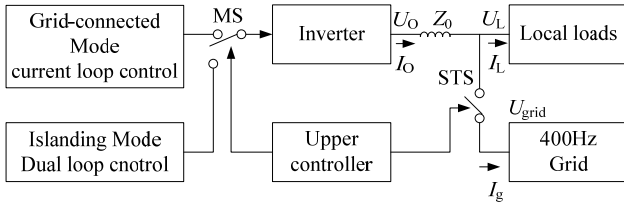
Fig. 3. Principle of the on/off-grid process of the 400-Hz solid-state power supply with local loads.

by setting RUN at "1." In the off-grid process, RUN is first set to "0" to block the PWM pulse, and the STS is turned off. At this time, the power supply is off-grid and stops running. In the above process, the grid unit is not involved in the on- or off-grid process because of its independent operation. With its relatively fixed switching sequence, the grid unit itself has a single working mode. The performance of the transient process depends entirely on the control strategy.

B. On/Off-Grid Process with Local Loads

Figure 3 shows the principle of the on/off-grid process of the 400-Hz solid-state power supply with local loads. In this case, the grid unit must operate in a grid-connected mode and in an islanding mode according to instructions. In addition, the two kinds of mode switching must be smooth. MS denotes the mode switch. U_O and I_O are, respectively, the output voltage and current of the grid unit. U_L and I_L are, respectively, the voltage and current of local loads. I_g is the current fed into the grid. The grid unit is under the voltage and current closed-loop control when it operates in islanding mode, namely, the output mode of voltage source. The grid unit is only under current single-loop control when it operates in a grid-connected mode, namely, the output mode of current source. STS controls the on/off-grid of the grid unit output. The upper controller controls the grid unit switching between the closed dual-loop and single-loop control modes by MS. In this paper, the sinusoidal pulse width modulation (SPWM) and MS controls are all based on digital signal processor (DSP).

Before STS is turned on, the grid unit of the 400-Hz solid-state power supply operates in an islanding mode, and the multi-ply dual-loop proportional-resonant (MDLPR) control is used in the unit. Furthermore, the grid unit supplies power to local loads, detects the zero-crossing voltage, and tracks the grid voltage phase by digital phase locked loop (PLL). When the upper controller gives an on-grid instruction, the control strategy of the grid unit converts to current single-loop control. Then STS is turned on to connect the grid unit to the grid at the zero-crossing of grid voltage, which then converts the operation mode of the grid unit to the grid-connected mode. In this operation mode, the grid unit output power is supplied to the local loads, and the rest is fed to the grid loads. When the upper controller gives an off-grid instruction, STS is turned off to make the grid unit convert to
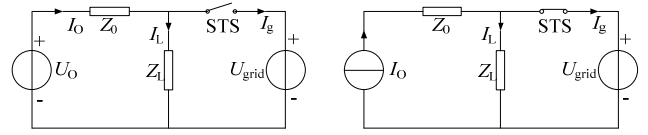

Fig. 4. Equivalent circuit of islanding and grid-connected operation mode of the grid unit.

the MDLPR control mode according to the control strategy. In this case, the grid unit operates in an islanding mode and supplies power to the local loads constantly.

In the on/off-grid process, a large voltage or current shock may happen, which is bad for the grid, loads, and power supply itself. Theoretically, the impact on the grid is the minimum when MS and STS are turned on/off synchronously. However, in the practical process, MS and STS can hardly achieve synchronization because of the time delay of the system and the switch. Therefore, a clear control sequence must be given, which can be determined through the analysis of mode switching transient process.

III. Analysis of Mode Switching Process of Grid-Connected System

Figure 4 shows the equivalent circuit of the grid unit operating in an islanding or grid-connected operation mode. Z_L is the local load. The following is the analysis of two kinds of mode switching transient process: one wherein MS is turned on/off before STS, and another where STS is turned on/off before MS.

A. MS Turned On/Off Before STS

Figure 5 shows the on-grid mode switching process of the power supply when MS is turned on before STS. t_1 and t_2 are, respectively, the initial time of MS and of STS. Before t_1, the grid unit supplies the load independently in the MDLPR control mode (voltage source). At t_1, MS is turned on and the grid unit is switched to the current single-loop control mode (current source), while STS remains off before t_2, with the result that a mode-switching transient state appears between t_1 and t_2. Before t_1, the PLL tracking control results in $U_L = U_{grid}$. The grid unit output current I_O depends on the local load Z_L, or $I_O = I_L$. At t_1, in most severe cases (I_{ref} is directly set to the average current without adjustment), the sudden change of I_O can lead to the grid current reference I_{ref}, or $I_O = I_{ref}$. At the moment, between t_1 and t_2, STS is off. Here, the full feeding of I_O into Z_L causes an amplitude of load voltage U_L to overshoot. U_L is expressed as follows:

$$U_L = I_{ref}Z_L \tag{1}$$

As U_L in (1) is limited by the power supply DC voltage, its overshoot is restricted, and I_O has limited distortion. At t_2, STS is turned on and the grid unit is switched to current single-loop control mode. The whole system operates in a grid-connected mode. At this time, the current loop reference
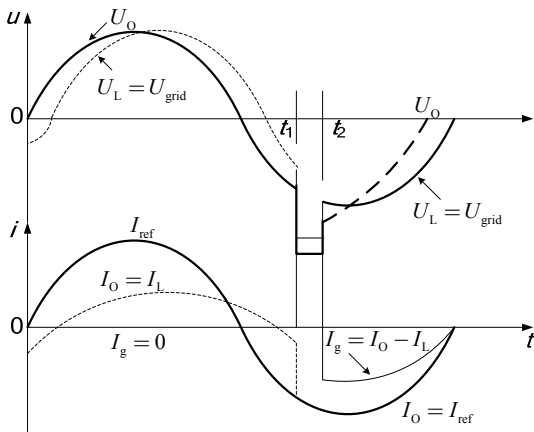
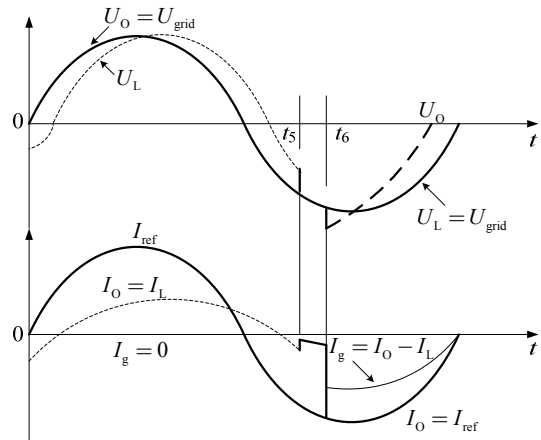Fig. 5. On-grid mode switching process of the 400-Hz solid-state power supply with MS turned on before STS.
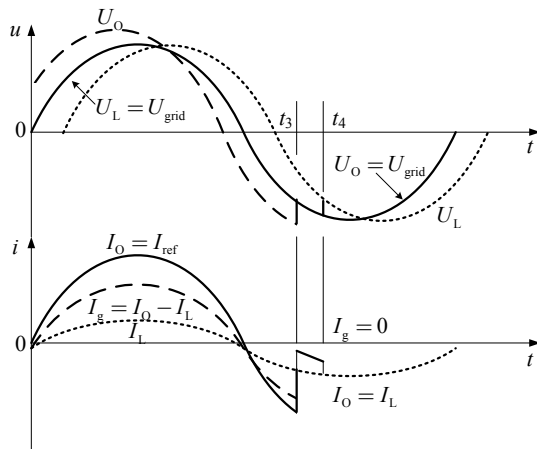

Fig. 6. Off-grid mode switching process of the 400-Hz solid-state power supply with MS turned off before STS.

remains the same and U_L is forced to drop to U_{grid}. I_O flows into Z_L to keep the grid unit working normally, and the rest is fed into the grid.

The expression is as follows:

$$\begin{cases} I_L = U_{grid} / Z_L \\ I_g = I_O - I_L \\ U_O = U_{grid} + I_O Z_0 \end{cases} \tag{2}$$

Figure 6 shows the off-grid mode-switching process of the power supply in the case of MS being turned off before STS. In the off-grid process, MS is turned off at t_3, at which the control of the grid unit changes from current single-loop control mode to the MDLPR control mode. However, given that STS remains closed, both the grid unit and the grid connected in parallel are in a transitional state of the load current. Here,

$$\begin{cases} U_L = U_{grid} \\ I_O = I_{ref} \\ I_g = I_O - I_L \end{cases} \tag{3}$$

From t_3 to t_4, STS is still on. The PR regulator of the grid unit voltage loop reaches the saturation value, and a transient circulation is easy to form because U_L is still clamped by U_{grid}. At t_4, STS is turned off. The PR regulator of voltage loop is out of saturation state because U_L is not clamped by U_{grid}. At this time, the grid unit operates in an islanding mode to supply power to local loads continuously.

B. STS Being Turned On/Off Before MS

Figure 7 shows the on-grid mode-switching process of the 400-Hz solid-state power supply at a time when STS is turned on before MS. When STS is turned on at t_5, U_L is immediately clamped to U_{grid}. As MS is off-state, the grid unit still operates in a MDLPR control mode of voltage source. The transitional process between t_5 and t_6 in Fig. 7 and that between t_3 and t_4 in Fig. 6 are the same. At t_6, MS is turned on, and the grid unit is switched to current single-loop control mode. The whole system goes into a grid-connected operating state with the load voltage staying constant. Consequently, Expression (2) still holds.

Figure 8 shows the off-grid mode switching process of the 400-Hz solid-state power supply under the condition of STS being turned off before MS. In the off-grid process, at t_7 STS is turned off before MS, and MS remains closed before t_8. I_{ref} is set to the local load current to make I_g equal to 0, and the grid unit keeps working in a current source control mode. I_O is all fed to the local load. Hence, the transient process is the same as the process between t_1 and t_2 shown in Fig. 1. At t_8, MS is off and the grid unit starts to supply power to the local load by using MDLPR control.

According to the above analysis, when STS is first turned on in the on-grid process or MS is first turned off in the off-grid process, a small sudden change will form a circulating-current impact, which constitutes a latent danger to safety. In addition, the saturation effect of the MDLPR control will cause the power supply to bear a large impact. On the contrary, if MS is first turned on in the on-grid
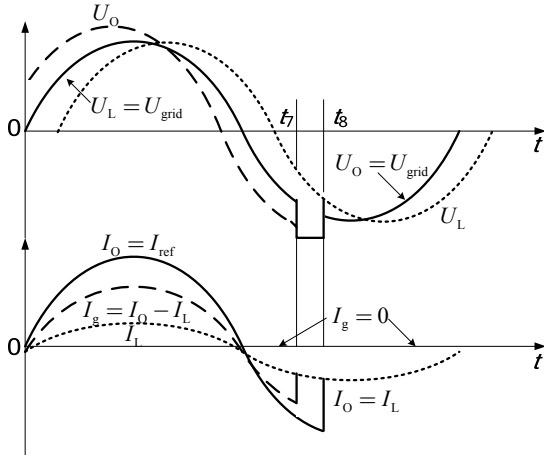
Fig. 8. Off-grid mode switching process of the 400 Hz solid-state power supply with STS turned off before MS.

process or STS is first turned off in the off-grid process, the sudden change that appears many times in load voltage will not threaten the safety of the grid unit due to the limit of the DC voltage. Hence, the power supply works relatively stable in the transient process.

Therefore, MS must be turned on before STS in the on-grid process, and STS must be turned off before MS in the off-grid process for the grid-connected 400-Hz solid-state power supply system.

IV.   MODE-SWITCHING SMOOTH CONTROL OF GRID-CONNECTED SYSTEM

The switching sequence of MS and STS is determined according to transient analysis. However, the key to a smooth transition with a smaller current shock in the on/off-grid process depends on the mode-switching control of the transient process of the grid-connected system. For this purpose, a mode-switching smooth control of the grid-connected 400-Hz solid-state power supply system is presented. Based on the grid-connected system shown in Fig. 9, an analysis is made of the highlights of its mode-switching smooth control.

In Fig. 9, G_f represents the low pass filter; K_U is the feedback gain of the grid voltage; $UpCmd$ is the command of MDLPR by the upper controller; I_{ad} is the current reference regulator of the grid unit; Z is the load impedance; U_{grid} and I_{grid}, respectively, are grid voltage and grid current; U_{grid_pk}, I_{grid_pk}, and I_{grid_RMS}, respectively, are grid voltage peak, grid current peak, and effective value; U_1 and U_2, respectively, are the voltage of grid units 1 and 2, I_{1_pk} and I_{2_pk}, respectively, are the current of grid units 1 and 2; F_m is the modulation ratio of DSP; UC&CG is the logic and digital calculation module of the upper controller; PK is the peak current calculation module; and D-DPLL is the discrete digital phase locked loop. As shown in Expression [4], the MDLPR control
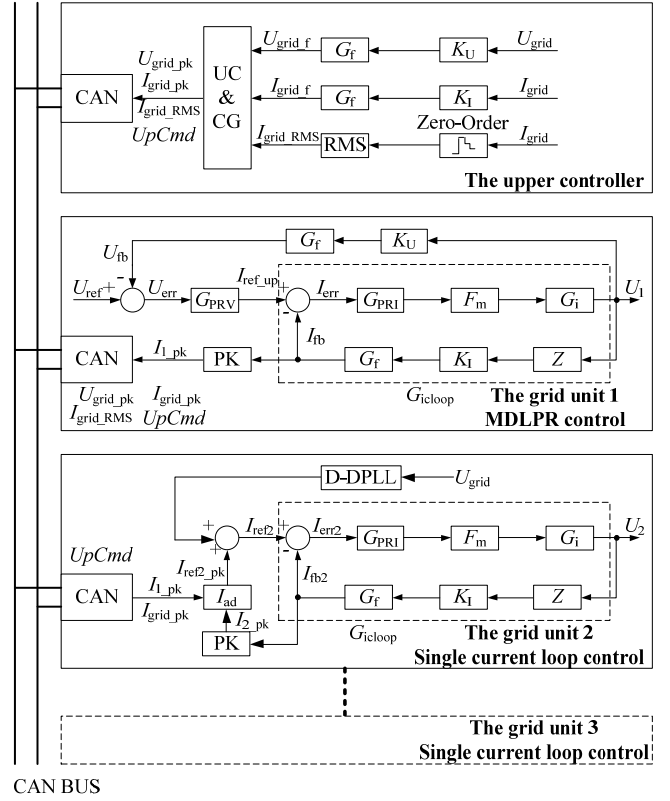
CAN BUS

Fig. 9. Grid-connected 400-Hz solid-state power supply system.

includes G_{PRV} and G_{PRI}, which are the voltage PR controller and the current PR controller, respectively [18]–[19].

$$\begin{cases} G_{PRV} = K_{pv} + \displaystyle\sum_{n=1,3,5...} \frac{K_{ivn}s}{s^2 + 2\omega_c s + (n\omega_0)^2} \\ G_{PRI} = K_{pi} + \displaystyle\sum_{n=1,3,5...} \frac{K_{iin}s}{s^2 + 2\omega_c s + (n\omega_0)^2} \end{cases} \quad (4)$$

where, K_{pv} and K_{pi} are proportional coefficients, which determine the speed of the system transient response to the step input signal. K_{ivn} and K_{iin} are fundamental frequency coefficients, which determine the response to the sinusoidal signal at the fundamental frequency. ω_0 is the fundamental angular frequency, and ω_c is the cut-off frequency of the DC compensator.

As shown in Fig. 9, each independent 400-Hz solid-state power supply has a DSP control system. The upper controller is responsible for the operation mode of the power supply and the current reference of the grid units. When the power supply switches from islanding mode to grid-connected mode, the first grid unit stays under the same control and the other grid units are switched from MDLPR control mode to current single-loop control mode. In the grid connection, at least one grid unit is operating in the MDLPR control mode, whereas the others are running in current single-loop control mode. The selection of a grid unit running in the MDLPR control or current single-loop control mode is determined by the upper controller through the controller area network (CAN) bus.

The communication channel will survive even when one node is disconnected with the hot-swap CAN bus. In addition, when the original MDLPR control unit fails, the grid-connected system can still operate because the upper controller will order another unit to work in the MDLPR control mode, thereby keeping the whole system running.

To reduce the circular current of the system, the grid-connected system must efficiently share the current among the grid units. As shown in Fig. 9, the upper controller orders the master unit to run in the MDLPR control mode through $UpCmd$ and shares out $I_{\text{grid\_pk}}$ calculated by UC&CG among all grid units through the CAN bus. The current peak value $I_{\text{ref2\_pk}}$ is determined by $I_{\text{grid\_pk}}$, $I_{\text{1\_pk}}$, and $I_{\text{2\_pk}}$ through I_{ad}. Regulation is conducted as follows:

$$I_{\text{ref 2\_pk}} = \frac{1}{N} I_{\text{grid\_pk}} + I_{\text{pk\_offset}}$$
$$I_{\text{pk\_offset}} = I_{\text{1\_pk}} - I_{\text{2\_pk}} \tag{5}$$

The constraints of (5) are

$$\begin{cases} I_{\text{pk\_offset}} = I_{\text{pk\_offset}}, & \left| I_{\text{1\_pk}} - I_{\text{2\_pk}} \right| < \Delta I_{\text{pk}} \\ I_{\text{pk\_offset}} = I_{\text{pk\_offset}} + I_{\text{pk\_step}}, & \left| I_{\text{1\_pk}} - I_{\text{2\_pk}} \right| > \Delta I_{\text{pk}} \end{cases} \tag{6}$$

In (5) and (6), N is the sum of the grid units. $I_{\text{pk\_step}}$ is the magnitude step size used to modify the magnitude offset of the grid units $I_{\text{pk\_offset}}$. In actual DSP calculation, $I_{\text{pk\_step}}$ is used for the PI regulation of $I_{\text{pk\_offset}}$. ΔI_{pk} is the constrained range of the difference of peak current. The regulating process above, called, "reactive power magnitude regulation," ensures smooth regulation of the current.

Similarly, the current phase reference $I_{\text{ref2\_}\theta}$ is determined both by output current phase $I_{\text{pll\_}\theta}$ through discrete digital phase locked loop (D-DPLL) and by voltage U_{2_θ} of the slave unit. The expression is as follows:

$$I_{\text{ref 2\_}\theta} = I_{\text{pll\_}\theta} + I_{\theta\_\text{offset}}$$
$$I_{\theta\_\text{offset}} = U_{2\_\theta} - I_{\text{pll\_}\theta} \tag{7}$$

The constraints of (7) are

$$\begin{cases} I_{\theta\_\text{offset}} = I_{\theta\_\text{offset}}, & \left| U_{2\_\theta} - I_{\text{pll\_}\theta} \right| < \Delta I_{\theta} \\ I_{\theta\_\text{offset}} = I_{\theta\_\text{offset}} + I_{\theta\_\text{step}}, & \left| U_{2\_\theta} - I_{\text{pll\_}\theta} \right| > \Delta I_{\theta} \end{cases} \tag{8}$$

In (7) and (8), I_{θ_step} is the phase step size used to modify the phase offset of the grid units I_{θ_offset}. In actual DSP calculation, I_{θ_step} is used for PI regulation of I_{θ_offset}. ΔI_{θ} is the phase band for the inequality case. The regulating process above guarantees smooth adjustment of the phase and is called, "active power phase adjustment."

From (5) and (7), the slave unit current reference is expressed as follows:

$$I_{\text{ref 2}} = I_{\text{ref 2\_pk}} \times I_{\text{ref 2\_}\theta} \tag{9}$$

By applying the above expression to the n^{st} unit, the current reference is expressed as follows

$$I_{\text{ref } n} = I_{\text{ref } n\_\text{pk}} \times I_{\text{ref } n\_\theta} \tag{10}$$

where

$$I_{\text{ref } n\_\text{pk}} = \frac{1}{N} I_{\text{grid\_pk}} + I_{\text{pk\_offset}} \qquad I_{\text{ref } n\_\theta} = I_{\text{pll\_}\theta} + I_{\theta\_\text{offset}}$$
$$I_{\text{pk\_offset}} = I_{\text{1\_pk}} - I_{n\_\text{pk}} \qquad\qquad I_{\theta\_\text{offset}} = U_{n\_\theta} - I_{\text{pll\_}\theta}$$

Although the control strategy can smoothly adjust the peak current and phase, its performance is insufficient. As shown in Fig. 3, the grid-connected 400 Hz solid-state power supply should either supply power to the local load or exchange the power with the 400-Hz grid. To continue supplying power to the local load, the grid unit must switch between the islanding and grid-connected modes without drastic electrical stresses. The mode-switching smooth control must follow the laws. First, the appearance of a large load voltage shock and a large magnitude of current during the switching time should be avoided. Second, the grid unit output voltage should match the grid voltage synchronously in magnitude, phase, and frequency before STS is closed.

Therefore, as shown in Fig. 9, the proposed steps of changing the grid unit from an islanding mode to a grid-connected mode are summarized as follows:

1) The upper controller monitors the U_{grid} to judge whether it will meet the requirement of the grid. By the real-time calculation of $U_{\text{grid\_pk}}$, $I_{\text{grid\_pk}}$, and $I_{\text{grid\_RMS}}$, the upper controller sends information to each grid unit through the CAN bus.
2) The grid unit output voltage should be matched with the grid voltage synchronously in magnitude, phase, and frequency by D-DPLL.
3) As soon as the slave grid unit receives the on-grid command $UpCmd\_1$ sent by the upper controller through the CAN bus, MS is firstly turned on. Thus, the slave grid unit can change from the MDLPR control mode to the current single-loop control mode. Its given value of output current is $I_{\text{ref}n\_\text{pk}}$.
4) STS should be turned on at the zero-crossing point of the grid voltage.
5) The synchronous regulation of $I_{\text{ref}n\_\text{pk}}$ and $I_{\text{ref}n\_\theta}$ according to (5) and (7) ensures that the grid unit tracks the grid synchronously.

Similarly, the proposed steps of changing the grid unit from the grid-connected mode to the islanding mode are summarized as follows:

1) The upper controller judges the operating conditions of the grid by monitoring U_{grid} and I_{grid} and sends the off-grid command $UpCmd\_0$ through the CAN bus.
2) To minimize the impact of current I_{g} fed into the grid, the slave grid unit should reduce the output current $I_{\text{ref}n\_\text{pk}}$ to the local load current.
3) STS should be turned off at the zero-crossing point of the grid voltage.
4) MS is turned off, and the slave unit is converted from the current single-loop control to the MDLPR control mode.

V. EXPERIMENTAL RESULTS

In this paper, the prototype of the grid-connected 400-Hz solid-state power supply system with three 100 kVA and 115 V/400 Hz power supply is used for simulative and experimental analysis, as shown in Fig. 10. Experimental conditions include DC-link voltage 600 V, capacitor of output 166 uF, inductance of output 100 uH, transfer ratio of transformer 292/115, modulation ratio 0.8, and switching frequency 10 kHz. One of the power supplies used for the master grid system runs in the MDLPR control mode.

Figure 11 shows simulation results of the on-grid process of the 400 Hz solid-state power supplies without local loads. Fig. 11(a) shows the results of the grid voltage, current, and grid unit current. The waveforms of the on-grid process begins at 20 ms, and grid voltage U_{grid} is recovered at 30 ms (The dynamic recovery time is 10 ms). The master power supply current i_{11} (I_{grid}) changes from 297 A to 100 A. The currents of two slave grid units are, respectively, 97.6 A and 99.4 A. Fig. 11(b) shows the circular current of phases A, B, and C. According to the waveforms, the peak transient circular current is less than 100 A, and the steady circular current is just 3.5 A. These currents satisfy the needs of the system.

Figure 12 shows simulation results of the on/off-grid process of phase A of the 400-Hz solid-state power supplies with local loads in an incorrect switching sequence. Fig. 12(a) shows that STS is turned on at 0.02 s and MS is turned on at 0.03 s (STS is turned on before MS). The grid voltage U_{grid} and the grid unit voltage U_{O1} have little fluctuation, but the shock of I_g is large, which causes the grid system to fail. As shown in Fig. 12(b), MS is turned off at 0.08 s and STS is turned on at 0.09 s (MS is turned off before STS). I_g increases immediately to several thousand amperes, which leads to a large distortion of grid unit voltage U_{O1}. Fig. 12 indicates that the transient process is the same as the analysis made in Section III.

Figure 13 shows simulation results of the on/off-grid process of the grid-connected 400-Hz solid-state power supply system with local loads under the mode-switching smooth control. Consider the waveforms of phase A as an example. In Fig. 13(a), MS is turned on at 0.02 s and STS is turned on at 0.03 s (MS is turned on before STS) in the on-grid process. The waveforms from top to bottom are, respectively, grid voltage U_{grid}, slave grid unit voltage U_{O1}, grid current I_{grid}, grid unit current I_{O1}, and local load current I_L. The grid unit current is fed into grid I_g. I_{grid} is 290.6 A when the grid operates with full-load, and I_{O1} is 145.3 A when the slave grid unit operates with half-load before the grid connection. Between 0.02 s and 0.03 s, U_{grid} and I_g remain constant because the slave grid unit is not connected to the grid. At 0.02 s, fluctuation appears in U_{O1}, I_{O1}, and I_L, and dampens gradually. The reason for such movement is that the slave grid unit changes from the MDLPR control mode to the

Fig. 10. Prototype of the grid-connected 400-Hz solid-state power supply system.
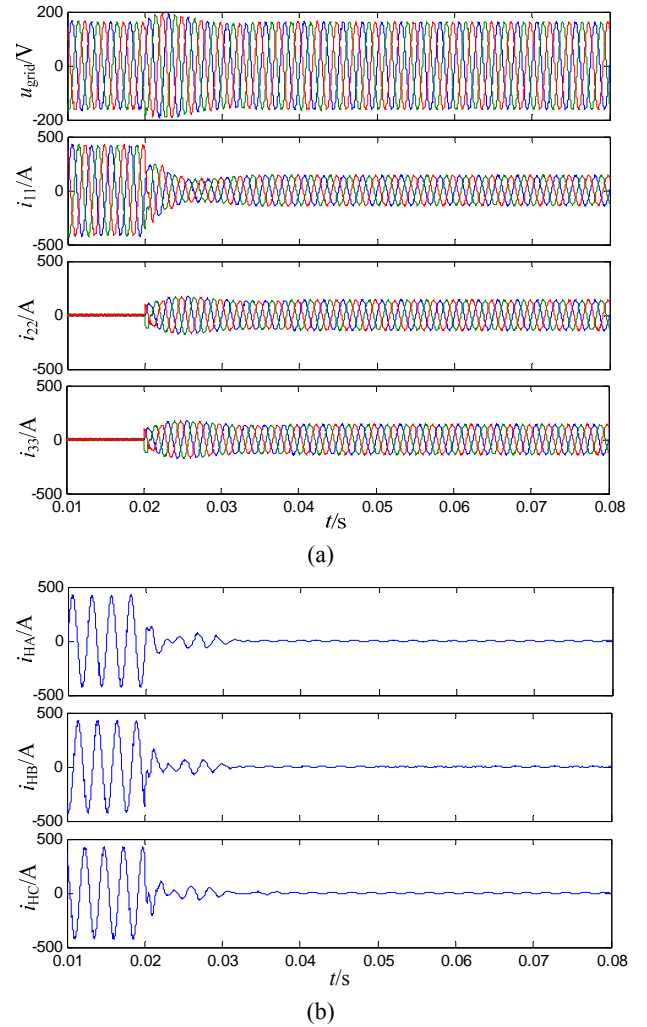

(a)

(b)

Fig. 11. Simulation results without local loads. (a) Grid voltage, current, and grid unit current. (b) Circular current of phases A, B, and C.

current single-loop control mode. Moreover, the current reference value abruptly changes into the grid current value. I_{O1} is all fed into the local load, but DC restrains the voltage shock. Hence, the results are identical to those of the theoretical analysis. U_{O1} is reduced to U_{grid} when STS is
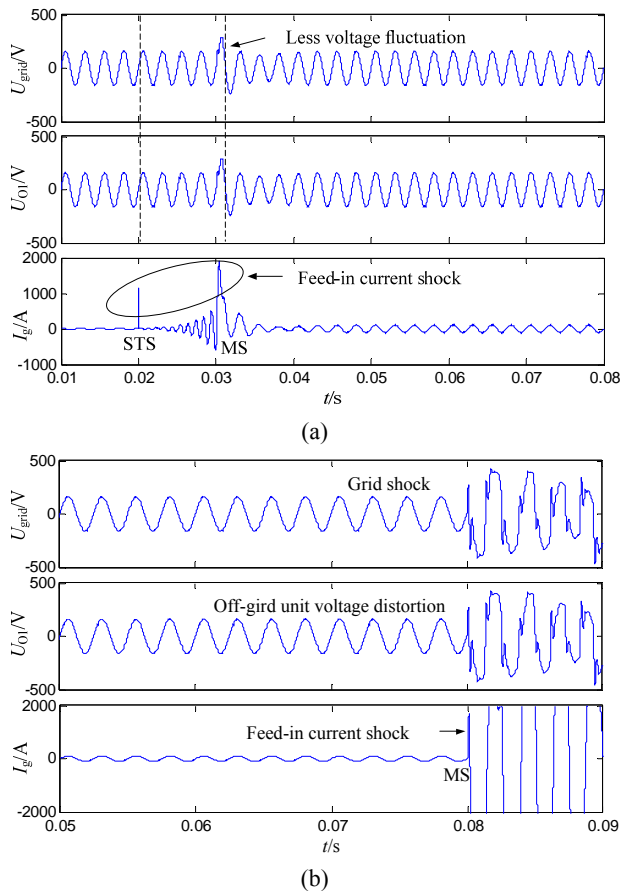
(a)

(b)

Fig. 12. Simulation results with local loads in a wrong switching sequence. (a) STS is turned on before MS. (b) MS is turned off before STS.

turned on at 0.03 s. Part of I_{O1} continues to supply power to the local load, and the rest is fed into the grid when I_{O1} changes from 145.3 A to 219.2 A. At the same time, I_{grid} changes from 290.6 A to 218.9 A. Then I_{O1} shares the grid current with I_{grid}. The comparison of Fig. 13(a) with Fig. 12(a) shows that the fluctuations of U_{grid} and U_{O1} increase. However, the system runs steadily throughout the transient process, and the peak I_g is only at 230 A with a small shock. Moreover, I_g is 73.6 A in the stable operation, supplying power to the grid loads.

As shown in Fig. 13(b), STS is turned off at 0.08 s and MS is turned off at 0.09 s (STS is turned off before MS) in the off-grid process.

The waveforms from top to bottom are the same as those in Fig. 13(a). The slave grid unit current reference value is reduced to the local load current value at 0.078 s before STS is turned off. The shock of I_g can be restrained when STS is turned off, as shown by I_{O1} and I_g waveforms in Fig. 13(b). U_{grid}, I_L, and U_{O1} barely change between 0.08 s and 0.09 s. Meanwhile, I_g decreases to 0, and I_{O1} changes from 219.2 A to 145.3 A, and I_{grid} changed from 218.9 A to 290.6 A. After MS is turned off, the slave grid unit is switched from the current single-loop control mode to the MDLPR control
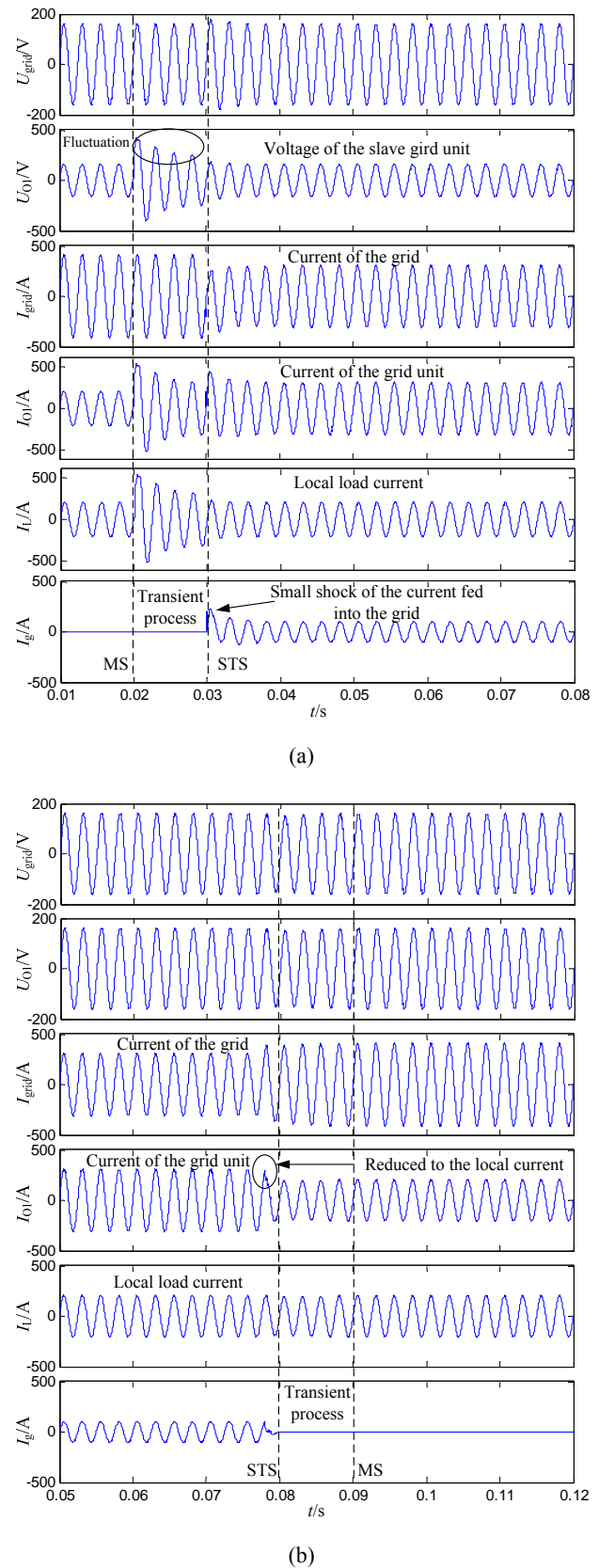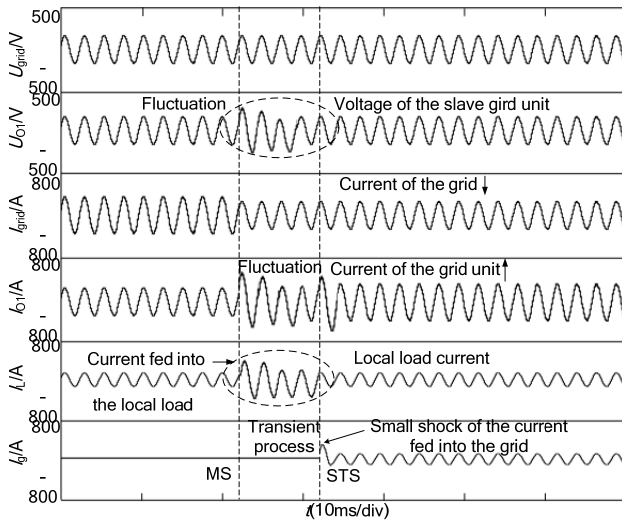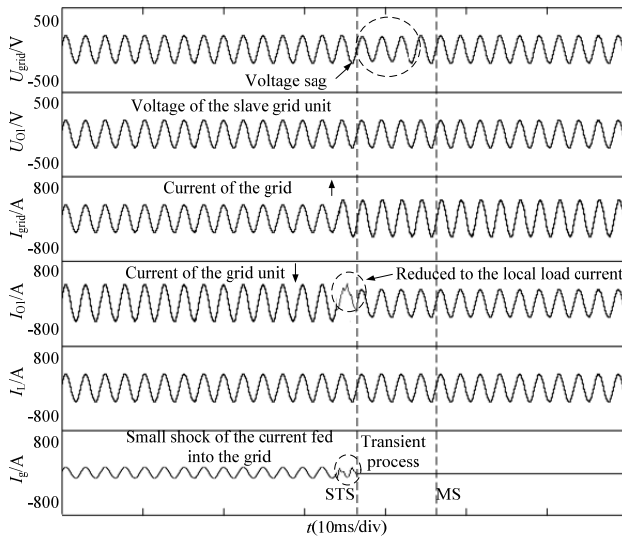

(a)

(b)

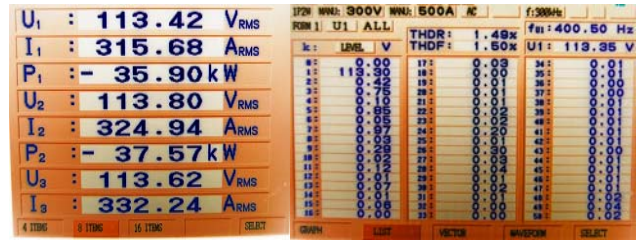Fig. 13. Simulation results with local loads under mode-switching smooth control. (a) On-grid process. (b) Off-grid process.

(a)

(b)

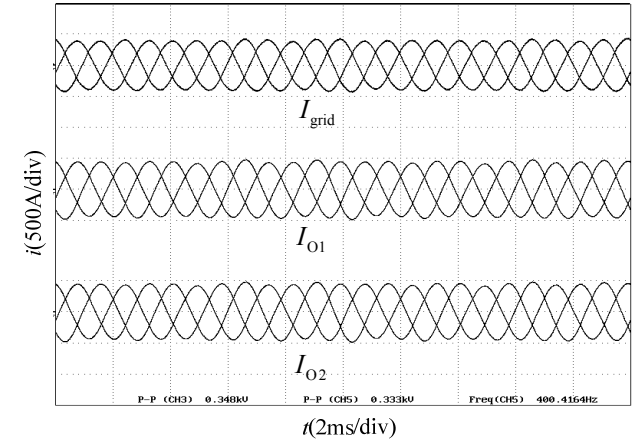Fig. 14. Experimental results with local loads under mode-switching smooth control. (a) On-grid process. (b) Off-grid process.

(a)   (b)

t(2ms/div)

(c)

t(2ms/div)

(d)

Fig. 15. Experiment results of the three grid-connected 100 kVA power supplies in the steady-state operation. (a) Output voltage and current of the grid. (b) Harmonic distribution. (c) Three-phase current of the grid and the unit. (d) Output current of the grid and the unit 2.

mode and continues to supply power to the local load. By comparing Fig. 13(b) with Fig. 12(b), the off-grid transient process is proved more stable.
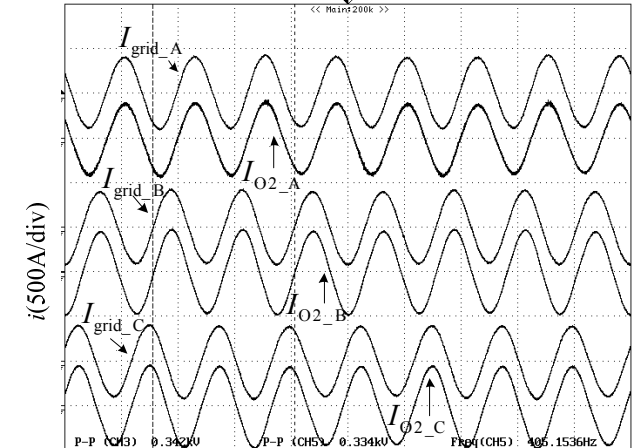
Fig. 14 shows the experiment results of the on/off-grid process of the grid-connected 400-Hz solid-state power supply system with local loads under mode-switching smooth control. Take the waveforms of phase A for example. As shown in Fig. 14(a), MS is turned on before STS in the on-grid process at the zero-crossing point of voltage. The waveforms from top to bottom are the same as the simulation waveforms. I_{grid} is 289.5 A when the grid is running with full-load, and I_{O1} is 144.8 A when the slave grid unit is running with a half-load before the grid connection. When MS is turned on and STS remains off (the dotted line regional), U_{grid} and I_g remain constant because the slave grid unit is disconnected from the grid. Fluctuations appear in

U_{O1}, I_{O1}, and I_L (the oval region) because the slave grid unit is switched from the MDLPR control mode to the current single-loop control mode, and the current reference value abruptly changes to the grid current value. Meanwhile, I_{O1} is all fed into the local load. I_{grid} decreases because of load overheating protection, which causes one of the grid loads to switch automatically off and on (normally, I_{grid} will remain still before STS turns on). Similar to simulation result, U_{O1} is reduced to the same value to U_{grid} when STS is turned on.

Part of I_{O1} continues to supply power to the local load, and the rest is fed into the grid when I_{O1} changes from 144.8 A to 218.7 A. Meanwhile, I_{grid} changes from 289.5 A to 219.4 A. Then I_{O1} shares the grid current with I_{grid}. The peak I_g is only 239 A with a small shock. Moreover, I_g is 71.2 A in stable operation, which supplies power to the grid loads.

As shown in Fig. 14(b), STS is turned off before MS is in the off-grid process (the dotted line regional). The slave grid unit current value is reduced to local load current value just one cycle earlier than the time when STS is turned off. I_{O1} and I_g waveforms indicate small fluctuations in the circular area that are similar to the case of the simulation. In the transient process, I_{grid} changes from 219.4 A to 289.5 A, and the peak U_{grid} has just a 3-volt drop when STS is turned off. Meanwhile, I_{O1} changes from 218.7 A to 144.8 A, and U_{O1} remains steady. The slave grid unit changes from current single-loop control to MDLPR control and continues to supply power to the local load.

Figures 13 and 14 show that the experimental results are highly consistent with the simulation results, thus proving that the theoretical analysis is correct and that the mode-switching smooth control is effective.

Figure 15 shows the experimental results of the three grid-connected 100 kVA power supplies in steady-state operation. The total output power is 333 kVA. As shown in Fig. 15(a), the grid output voltage is balanced under the condition of unbalanced loads, and the unit power reaches 111 kVA. Fig. 15(b) shows the R.M.S value, frequency, and the first 50 harmonic distributions of the grid voltage. The frequency of 400.5 Hz and the THD at 1.5% are suitable for the system. The three-phase output currents are shared efficiently, although the loads are unbalanced, as shown in Fig. 15(c). The comparison of the three-phase grid current with the current of grid unit 2 in Fig. 15(d) shows that the magnitude and phase are highly consistent.

VI. CONCLUSIONS

This study analyzed the operating principle of the grid-connected 400-Hz solid-state power supply and the related on/off-grid process with or without local loads. In addition, the theoretical study examined the effects of different switching sequences on the mode-switching transient process. The conclusion is that MS must be turned on before STS in the on-grid process and the STS must be turned off before MS in the off-grid process. A novel strategy for the mode-switching smooth control of the system was proposed and concrete steps were presented. The strategy aims to achieve a no-shock connected-grid through the average distribution of peak currents and the smooth adjustment of peak currents and phases. Simulations and experiments proved that the theoretical analysis is correct and that the method for smooth control is effective.

REFERENCES

[1] C. Li, S.-M. Ji, and D. P. Tan, "Multiple-loop digital control method for a 400-Hz inverter system based on phase feedback," *IEEE Trans. Power Electron.*, Vol. 28, No. 1, pp. 408–417, Jan. 2013.

[2] J. Zhu, Z. Nie, W. Ma, and S. Nie, "Comparison between DB control and dual-loop PR control for collapsed H-bridge single-phase 400Hz power supply," in *IEEE International Symposium on Industrial Electronics (ISIE)*, pp. 240-250, May 2012.

[3] H. Hu and Y. Xing, "Design considerations and fully digital implementation of 400-Hz active power filter for aircraft applications," *IEEE Trans. Ind. Electron.*, Vol. 61, No. 8, pp. 3823-3834, Aug. 2014.

[4] J. Liu, P. Zanchetta, M. Degano, and E. Lavopa, "Control design and implementation for high performance shunt active filters in aircraft power grids," *IEEE Trans. Ind. Electron.*, Vol. 59, No. 9, pp. 3604-3613, Sep. 2012.

[5] C. Liu, W. Ma, C. Sun, and W. Hu, "Digital control design of high power 400Hz inverters," *Transactions of China Electrotechnical Society*, Vol. 26, No. 1, pp. 100-107, Jan. 2011.

[6] N. Bottrell, M. Prodanovic, and T. C. Green, "Dynamic stability of a microgrid with an active load," *IEEE Trans. Power Electron.*, Vol. 28, No. 11, pp. 5107-5119, Nov. 2013.

[7] Q. Liu and M. Xie, "Strategies of grid-connection of doubly-fed variable-speed constant-frequency wind power generator with no-load and with load," *Transactions of China Electrotechnical Society*, Vol. 27, No. 10, pp. 60-68, Oct. 2012.

[8] S. Rivera, S. Kouro, B. Wu, S. Alepuz, M. Malinowski, P. Cortes, and J. Rodriguez, "Multilevel direct power control-A generalized approach for grid-tied multilevel converter applications," *IEEE Trans. Power Electron.*, Vol. 29, No. 10, pp. 5592-5604, Oct. 2014.

[9] C. T. Lee, R. P. Jiang, and P. T. Cheng, "A grid synchronization method for droop-controlled distributed energy resource converters," *IEEE Trans. Ind. Appl.*, Vol. 49, No. 2, pp. 954-962, Mar./Apr. 2013.

[10] J. M. Guerrero, T. L. Lee, P. C. Loh, and M. Chandorkar, "Advanced control architectures for intelligent microgrids - part II: Power quality, energy storage, and AC/DC microgrids," *IEEE Trans. Ind. Electron.*, Vol. 60, No. 4, pp. 1263-1270, Apr. 2013.

[11] J. Jiang, S. Duan, and Z. Chen, "Research on control strategy for three-phase double mode inverter," *Transactions of China Electrotechnical Society*, Vol. 27, No. 2, pp. 52-58, Feb. 2012.

[12] J. M. Guerrero and L. T. Lee, "Power quality in microgrids and distribution power systems," in *Proceedings of the ISIE*, pp. 978-986, May 2012.

[13] X. Tang, W. Deng, and Z. Qi, "Research on grid-connected islanded seamless transition of microgrid based on energy storage," *Transactions of China Electrotechnical Society*, Vol. 26, No. 1, pp. 279-284, Feb. 2011.

[14] X. Chen, Y. Z. Sun, and Z. Meng, "Design on stand-alone

grid-connected photovoltaic inverter system," *IEEE Trans. Power Electron.*, Vol. 46, No. 1, pp. 56-60, May 2012.

[15] X. Tang, W. Deng, and Z. Qi, "Investigation of the dynamic stability of microgrid," *IEEE Trans. Power Syst.*, Vol. 29, No. 2, pp. 698-706, Mar 2014.

[16] A. Eid, H. El-Kishky, M. Abdel-Salam, and M. T. El-Mohandes. "On power quality of variable-speed constant-frequency aircraft electric power systems," *IEEE Trans. Power Del.*, Vol. 25, No. 1, pp. 55–65, Jan. 2010.

[17] L. Zixin, W. Ping, and L. Yaohua, "400Hz high-power voltage-source inverter with digital control," in *Proceedings of the CSEE*, Vol. 29, No. 6, pp. 36-42, Feb. 2009.

[18] J. Zhu, W. Ma, Z. Nie, and Y. Wu, "Harmonic analysis and sectional suppression of 400Hz solid-state power supply," in *39th Annual Conference of the IEEE Industrial Electronics Society (IECON)*, pp. 802-807, Nov. 2013.

[19] J. Zhu, W. Ma, and Z. Nie, "Integration control based on droop characteristics achieving double synchronization with the switching signal and the reception phase," *High Voltage Engineering*, Vol. 42, No. 1, pp. 77-82, Jan. 2016.

Jun-Jie Zhu was born in China in 1984. He received his B.S., M.S., and Ph.D. in Electrical Engineering from Naval University of Engineering, Wuhan, China, in 2007, 2009, and 2013, respectively. From 2013 to 2015, he worked in the National Key Laboratory for Vessel Integrated Power System Technology, Naval University of Engineering as a Research Assistant. He is currently an Assistant Professor in National Key Laboratory for Vessel Integrated Power System Technology. His current research interests include power electronic converters, matrix converters, microgrids, distributed generation, and the application of power electronics in electromagnetic emission, harmonics, and power quality compensation systems.

Zi-Ling Nie was born in China. He received his B.S. (with honors), M.S., and Ph.D. degrees from Huazhong University of Science and Technology (HUST), China, in 1998, 2001, and 2005, respectively. He went to the University of Michigan in 2007 as a visiting scholar. Currently, he is a professor at Naval University of Engineering, China. His research interests include power electronics, high-voltage and high-power converters, HEV/EVs, and renewable energy. He has completed various projects with his teammates, such as those regarding electro-cars, medium frequency aviation power supplies, and motor excitation, to name a few.

Yin-Feng Zhang was born in China in 1983. He received his B.S. and M.S. in Air Force Early Warning Academy, China, in 2008 and 2011. Currently, he is studying his Ph.D. in National Key Laboratory for Vessel Integrated Power System Technology, Naval University of Engineering. His research interests include microgrids, distributed generation, and the control, design, and analysis of medium-frequency inverters. He is the author or coauthor of more than 10 technical papers in refereed journals and has presented in conferences.

Yi Han was born in China in 1990. Currently, he is studying his Ph.D. in National Key Laboratory for Vessel Integrated Power System Technology, Naval University of Engineering. He finished his research on efficiency optimization of high-current DC–DC converters based on synchronous rectification and joined a high-power aviation power supply project during his Master's study. At present, he is responsible for a project on medium-frequency AC and DC dual output aviation power supplies. His research plans mainly target motor control and AC drives.